Surface Science **666 (2017) 96–103**
http://dx.doi.org/10.1016/j.susc.2017.08.021

Growth and Phase Transformations of Ir on Ge(111)

C. H. Mullet,[1] B. H. Stenger, A. M. Durand,[2] J. A. Morad, Y. Sato,[3]
E. C. Poppenheimer,[4] and S. Chiang

Department of Physics
University of California Davis
1 Shields Avenue
Davis, CA 95616-5270, USA

Abstract:

The growth of Ir on Ge(111) as a function of temperature between 23°C and 820°C is characterized with low energy electron microscopy (LEEM), low energy electron diffraction (LEED), scanning tunneling microscopy (STM), and x-ray photoemission spectroscopy (XPS). Deposition onto a substrate at 350°C revealed a novel growth mode consisting of multilayer Ir islands with (√3 x √3)R30° (abbreviated as √3) structure interconnected by "bridges" of single-layer Ir several atoms wide. For deposition onto substrates above 500°C, the √3 Ir phase grows with dendritic morphology, and substrate step bunches act as barriers to √3 Ir growth. LEEM images showed Stranski-Krastanov growth for 650-820°C: after the √3 phase covers the surface, corresponding to 2 monolayers (ML) Ir coverage, multilayer hexagonal-shaped Ir islands form, surrounded by regions of IrGe alloy. Hexagonal-shaped Ir islands also formed upon heating 1.2ML of √3 Ir beyond 830°C, which resulted in the elimination of √3 structure from the surface. The transformation from √3 to (1x1) structure upon heating to 830°C was an irreversible surface phase transition. Annealing >2.0ML of Ir in the √3 phase above the 830°C disorder temperature, followed by cooling, produced a (3x1) structure. Subsequent heating and cooling through 830°C give evidence for a reversible (3x1) to (1x1) phase transition.

---

[1] Current address: Intel Corporation, Hillboro, OR, 97124
[2] Current address: Dept. of Physics, University of California, Santa Cruz, CA, 95064
[3] Current address: Gatan, Inc., Pleasanton, CA 94588
[4] Current address: Cambria, CA 93428

***Surface Science* 666 (2017) 96–103**
http://dx.doi.org/10.1016/j.susc.2017.08.021

Keywords: LEEM; LEED; Ir; Ge(111); surface phases

1. Introduction

Although many systems of metals on semiconductors have been previously studied because of applications to electrical contacts, the deposition of Ir on Ge has received comparatively little attention from surface studies. A recent study of Ir on Ge(001) found quantum size effects to be responsible for the growth of preferred lengths of iridium nanowires.[1] Iridium silicide nanowires have also been formed on both Si(001)[2, 3] and Si(110)[4] surfaces. Ring cluster structures have been observed for Ir on Si(111)[5] and result in the observed surface reconstruction.[6] The electronic properties and silicide formation for Ir deposited on Si have been of interest for applications to electrical devices.[7-14] Ir-Si layers have also been used for short wavelength UV mirrors for use in lithography tools.[15, 16]

For Ir on Ge, an earlier study examined the formation and diffusion of various iridium germanides, Ir_xGe_y, that are created when a thin film of Ge is deposited on a thin film of Ir and annealed to 350-800°C.[17] Another study examined the deposition of 20 transition metals, including Ir, on both amorphous Ge and Ge(001) in an effort to identify metals to use for electrical contacts on Ge-based microelectronics.[18] This study found that a 30 nm Ir film deposited on Ge(001) begins to form binary compounds with Ge at temperatures T ≥ 600°C but did not examine lower coverage of Ir. We are not aware, however, of published studies about the deposition of Ir on Ge(111).

We used low energy electron microscopy (LEEM), low energy electron diffraction (LEED), and scanning tunneling microscopy (STM) to characterize the growth of Ir on Ge(111) as a function of coverage, deposition temperature, and annealing temperature. Most experiments were conducted at less than 4 monolayers (ML) coverage. For growth conducted at 350°C, we observed unique mesoscale ordering in STM images: multilayer islands of Ir interconnected by thin "bridges" of single layer Ir. Growth above 650°C was quite different, with LEEM movies showing multilayer island growth only after the completion of a (√3x√3)R30° (abbreviated as √3) wetting layer. In addition, we observed the formation of a (3x1) phase after annealing and cooling.

2. Experimental details

Measurements were carried out in an ultrahigh vacuum (UHV) system consisting of three connected chambers housing several commercial instruments, including a LEEM (Elmitec GmbH), STM (Oxford Instruments), and x-ray photoemission (XPS) spectrometer (Vacuum Generators).[19] Ge(111) samples were cut from *n*-doped 2-inch commercial wafers that had a reported miscut <0.5°. Ge samples were cleaned with cycles of Ar^+ ion sputtering (250 eV, 5 μA) and annealing (800-830°C) until a sharp LEED pattern corresponding to the Ge(111) c(2x8) reconstruction was observed. The sample was heated using radiant and electron beam heating from a tungsten filament located behind the sample. The sample temperature was measured with a thermocouple in contact with the edge of the sample and calibrated to readings from an optical pyrometer that measured the sample temperature at the center of the sample. LEEM Data Analyzer software was used to analyze the LEEM data,[20] and WSxM software was used to analyze the STM data.[21]

Ir was deposited from a homebuilt evaporator attached to the LEEM sample chamber. A 97% pure Ir slug, 6.0 mm in length and 6.0 mm in diameter, with an initial mass of 3.8 g, was heated with electrons emitted by a hot tungsten filament and accelerated by a 3.5-4.5 kV potential on the Ir slug. The evaporator power was between 100 and 200 W. The evaporator was fitted with a shutter, operated with a rotary feedthrough, between the Ir source and the sample chamber. The shutter was opened to begin Ir deposition on the sample and closed to end the deposition.

3. Results and discussion

Results are discussed below for two different temperature ranges: Ir deposition on samples held at temperatures from room temperature (RT) to 500°C, and from 650 to 820°C. LEED confirmed that Ir growth from 340 to 500°C had the √3 structure, but domain sizes were too small to resolve with LEEM. STM images measured after Ir deposition at 350°C showed the growth of multilayer islands before the completion of a √3 wetting layer. From 650 to 820°C, Ir growth was observed in LEEM as large domains of the √3 phase, followed by multilayer island growth upon completion of the √3 layer, thus indicating a Stranski-Krastanov growth mode.[22] High temperature annealing of such samples causes the formation of compact, hexagonal Ir islands and transition to a (3x1) phase.

3.1. Calibration of Ir coverage using XPS

XPS calibration of Ir surface coverage was done through LEEM observation of the growth of the √3 Ir phase, discussed in more detail below. Ir was deposited for 17 minutes onto a Ge(111) substrate held at 610°C. The √3 phase was observed to completely cover the surface after 10 minutes of Ir deposition, followed by additional island growth. After the deposition of Ir, the XPS spectra of the sample were measured with Al Kα x-rays. Using CasaXPS software,[23] a Shirley background[24] was subtracted from the spectra, and the areas of the Ge 3d and Ir 4f peaks were measured. To determine the Ir coverage of the sample, the ratio of areas of the experimental peaks was compared with the ratio of areas of peaks in simulated spectra produced with Simulation of Electron Spectra for Surface Analysis (SESSA) software.[25] (Fig. 1). The XPS spectra of the sample were compared with the simulated data. The Ir thickness was determined to be 3.6 Å, corresponding to coverage of 3.5 ML and a dosing rate of 0.2 ML/min.

By comparing the deposition times, the completion of one layer of the Ir √3 phase observed by LEEM was therefore determined to correspond to Ir coverage of 2.0 ML from the XPS calibration. With the assumption that the deposition rate maintained a constant flux, this calibration was used to convert direct measurements of the completion of a layer of the √3 Ir phase in the LEEM images to ML for the data presented in this paper.

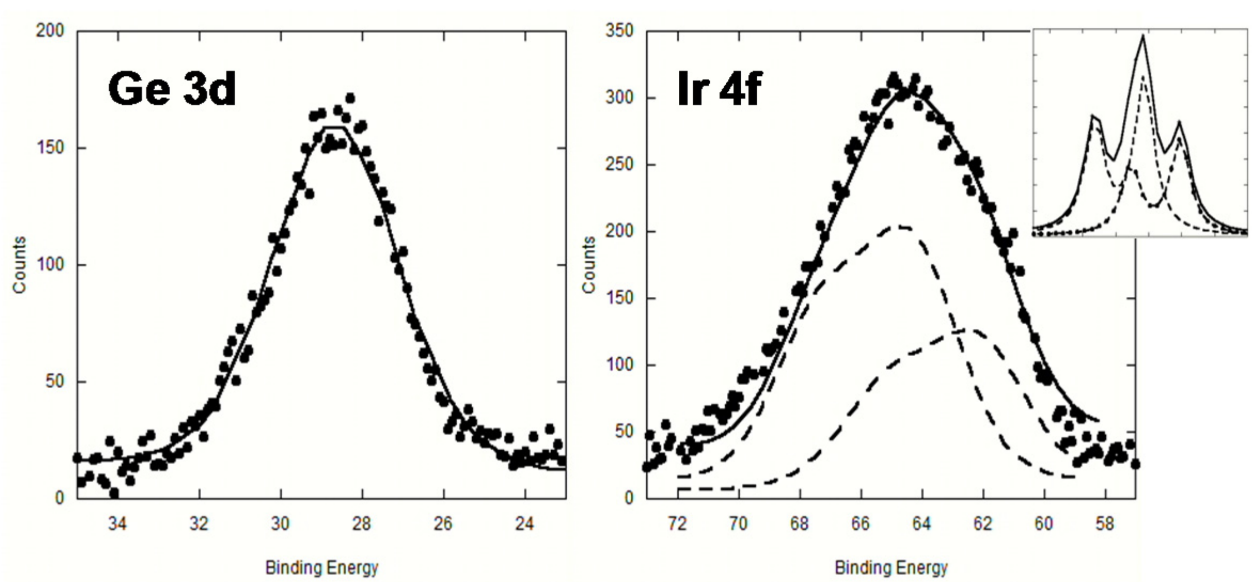

FIG. 1. Spectra of Ge 3d and Ir 4f peaks from measured XPS data of a Ge sample after 17 minutes of dosing with Ir. The solid lines correspond to simulated XPS spectra of 2 different layers on a Ge substrate, as described in the text. The two layers of Ir, with and without a chemical shift, each produce a doublet (dotted lines) which sum to the simulated Ir 4f spectrum. A Shirley background has been subracted from the measured data. The simulated spectrum of the Ge 3d peak is shifted in energy and convolved with a Gaussian function, with a full width half maximum of 2.6 eV, to account for the instrumental energy shift and resolution. Each Ir 4f spectrum was convolved with a Gaussian of the same width as was used for the Ge 3d peak. The two Ir 4f spectra and their sum before the convolution is shown in the inset. For both Ge and Ir peaks, the simulations were scaled to have the same areas under the curves as the corresponding data.

The asymmetric shape of the Ir 4f peak, with the shoulder on the right side and the unresolved spin-orbit doublet, indicated that two distinct species of Ir, with a chemical shift between them, were present on the surface. This shift can be explained by an increase in the binding energy of the first 2 ML layer of Ir, corresponding to the first complete layer of the √3 phase, due to bonding of the Ir atoms to Ge atoms within this layer. The lower binding energy species is likely to be more metallic Ir that forms islands above the initial layer.

With SESSA, we simulated an XPS spectrum consisting of 2 different layers on top of a Ge substrate: (1) 4 Å thickness with equal amounts of Ge and Ir, with a chemical shift of 2.2 eV applied to the Ir, and (2) 1.6 Å of Ir with no chemical shift, above the mixed Ir-Ge layer. To account for the instrumental resolution, a Gaussian with a full width half maximum of 2.6 eV was convolved with the simulated Ge 3d peak to give a good fit to the measured Ge 3d peak (Fig. 1, left side). The same Gaussian was then subsequently convolved with the Ir 4f spectra, which closely matched the measured XPS data after vertical scaling (Fig. 1, right side). The fit shown has a ratio of 1.6:1 for the higher binding energy doublet relative to the lower energy one. We determined, however, that the fit is not sensitive to small changes, either in the energy shift (≤0.4 eV) or in the fraction of Ir included in the energy shifted layer. Therefore, the exact parameters of the chemical shift cannot be determined. Nevertheless, a model with 2ML of Ir bonded to Ge,[26] giving a peak with larger area and increased binding energy, together with a smaller amount of metallic Ir in islands on top, can account for the shape of the Ir 4f peak in the measured XPS spectrum.

3.2. Growth of Ir on Ge(111) between room temperature and 500 °C: observation of novel √3 Ir phase

Figure 2 presents LEEM, LEED, and STM results for the deposition of 1.0 ML of Ir on Ge(111) at 350°C. The total reflectivity of the LEEM image changes upon Ir deposition, but otherwise there is no observation of new structures (Fig. 2b). The LEED pattern changes from Ge(111) c(2x8) (Fig. 2a) to √3 (Fig. 2c). STM images show large terraces of Ge(111) covered with islands ~5 nm in diameter (Fig. 2ef). Taken together, LEEM, LEED, and STM suggest that

Ir growth at 350°C is in the form of small islands of √3 Ir which are too small to resolve in LEEM images. For convenience, we henceforth refer to islands observed in STM or LEEM images that result from Ir deposition as "Ir islands", with the understanding that these islands may contain Ge as well as Ir. As described above, one previous study found that IrGe and Ir_4Ge_5 form when a Ge film was deposited on an Ir film and annealed at 350°C,[17] and other iridium germanides with various stoichiometry have been observed at higher temperatures up to 800°C.[17, 18]

Figure 3 presents higher resolution STM images of the same sample from which the LEEM image of Fig. 2(d) was measured. The smallest islands resolved in the STM images in Figure 3 are nearly 1 nm in diameter, ~1.0Å in height, and most likely correspond either to single Ir atoms or adatom clusters. For convenience, we will refer to these features as single Ir adatoms in the following discussion. In Figure 3a, Ir adatoms and single-layer clumps of Ir atoms cover approximately 20% of the surface, and approximately 15% of the area is covered by multilayer islands. There is a strong correlation between the lateral and vertical dimensions of multilayer islands. Most islands are between 3-6 nm in diameter and ~2.5Å in height. Several large islands, with diameters of 10-25 nm, range in height up to 6Å. Height measurements were calibrated to the Ge(111) double-step height, 3.3Å. The most probable interpretation of the height distribution is that islands 2.5Å in height correspond to two layers of Ir, and that the larger islands are composed of two or more layers of Ir. The lattice constant of bulk Ir is 3.84Å,[27] which gives an interlayer spacing of 2.2Å if islands were composed of Ir(111). Although the measured height of double-layer Ir islands, 2.5Å, is less than that obtained by adding the bulk Ir(111) interlayer spacing to the 1.0Å height that we observed for single Ir adatoms on Ge(111), the difference is small enough that it may be attributable to electronic effects.

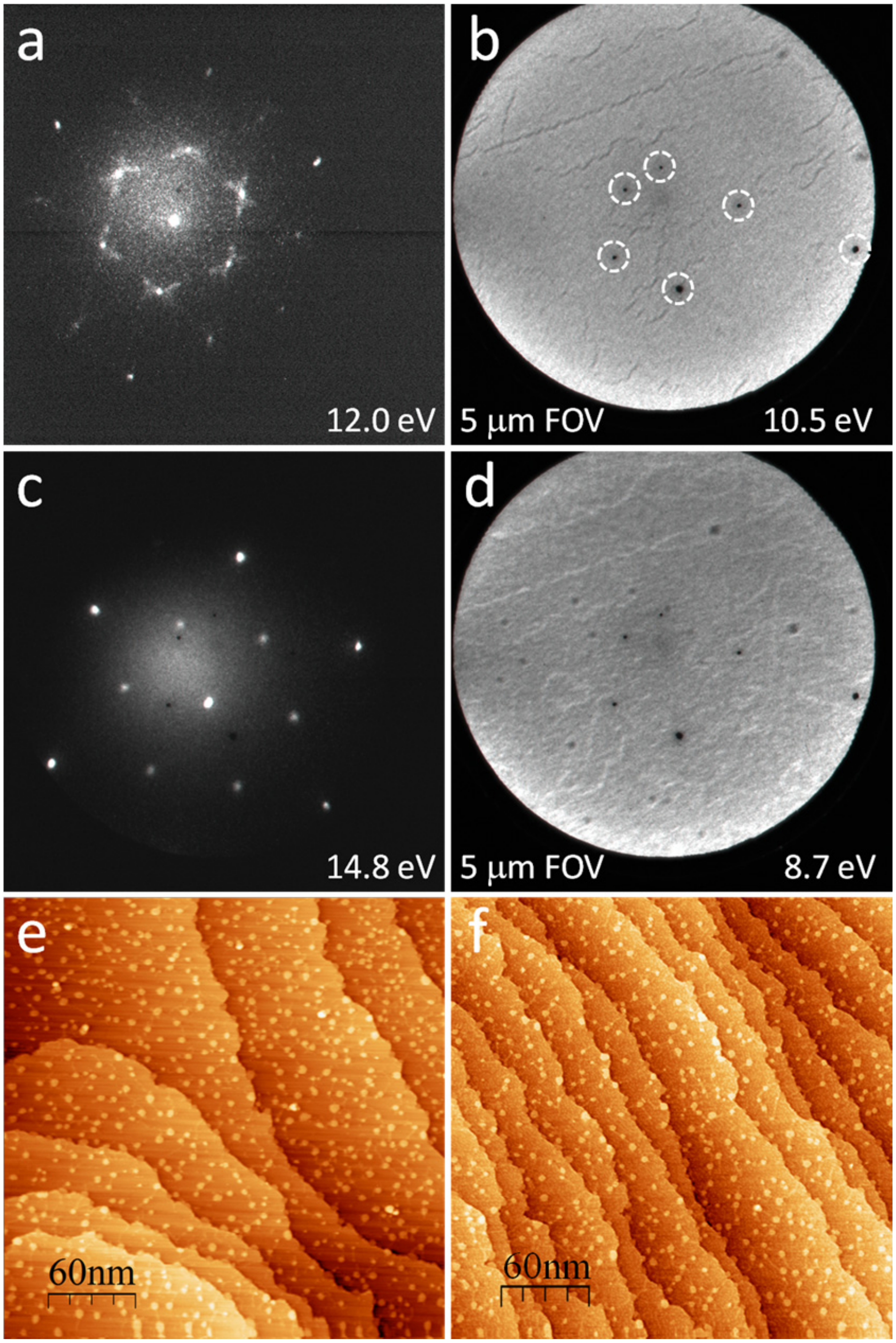

FIG. 2. LEED, LEEM (with field-of-view FOV indicated), and STM images before (a,b) and after (c,d,e,f) deposition of 1.0ML of Ir on Ge(111) at 350°C. (a) Clean Ge(111) c(2x8) LEED pattern before Ir deposition. (b) LEEM image of clean Ge(111) surface. Step bunches and surface defects are visible as dark contrast. Six black spots (enclosed in dotted circles) are burned into the LEEM channel plate, and are found in all LEEM images presented here. (c) Ge(111) √3-Ir LEED pattern after deposition. (d) LEEM image after Ir deposition. The total reflectivity of the entire surface has changed, and step contrast has reversed after deposition. Contrast around defects has increased. Changes in step and defect contrast from (b) are not due to the difference in imaging electron energy (data not shown) but rather to Ir deposition. Ir islands are too small to resolve in LEEM images. (e,f) STM images of Ir islands on Ge(111). Ir islands ~5 nm in diameter are found on Ge(111) terraces and at step edges. Sample bias= -2.0 V, tunneling current=0.5 nA.

Surface Science **666 (2017) 96–103**
http://dx.doi.org/10.1016/j.susc.2017.08.021

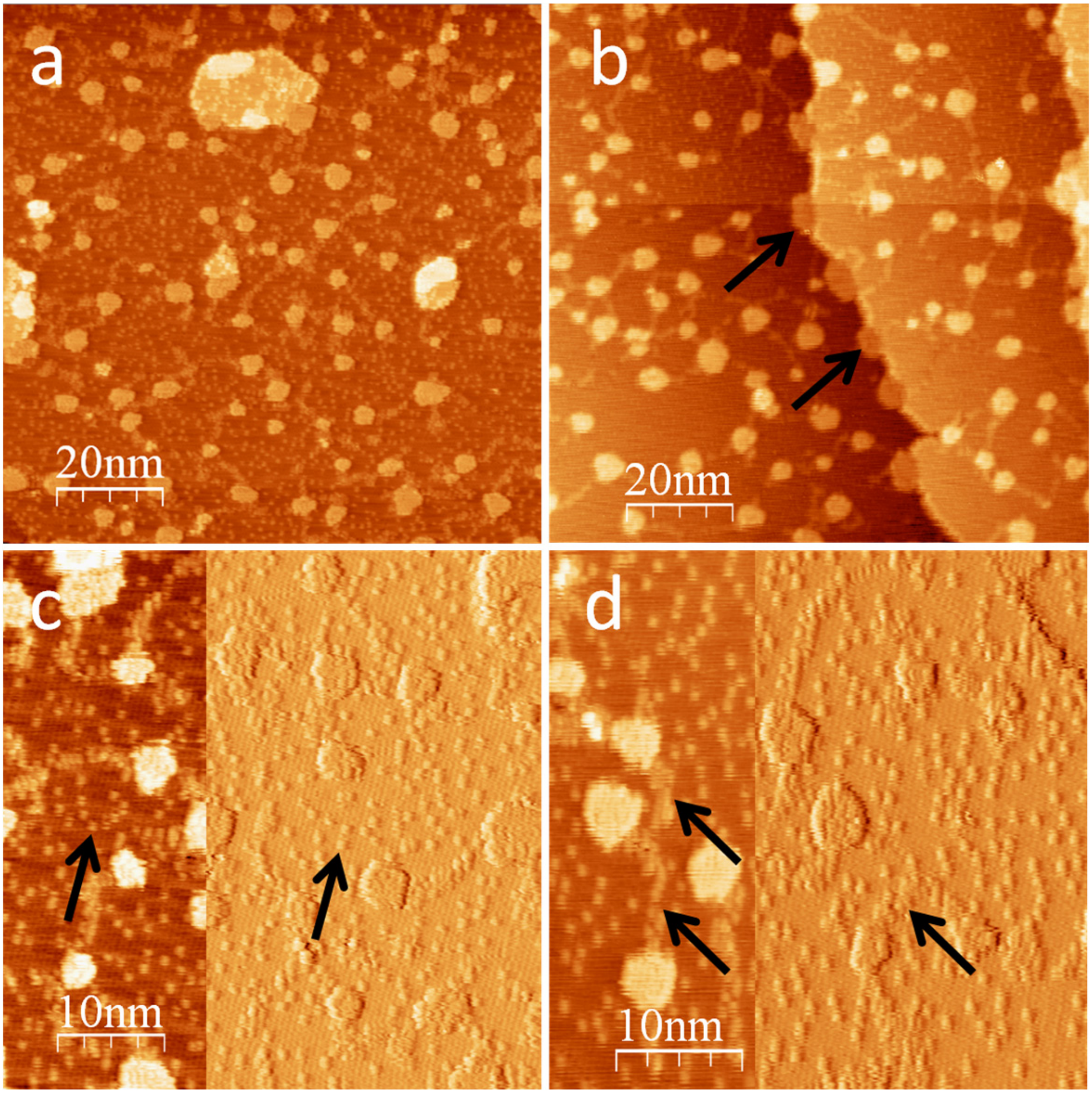

FIG. 3. (Color online) Room temperature STM image of 1.0ML of Ir deposited on Ge(111) at 350°C (LEEM image of same surface shown in Fig. 2d). Sample bias= -2.0 V, tunneling current=. 0.5 nA. The right-hand portion of the images in (c) and (d) have been differentiated to enhance contrast. (a) Single-layer Ir islands ~5 nm in width are observed, as well as larger multilayer islands. Clumps of Ir atoms form bridge-like structures between islands. (b) Ir islands are found on terraces and step edges but show a preference for growing on the lower edges of Ge(111) steps (arrows). (c) Arrows point to Ir adatoms and are oriented parallel to the Ge[$1\,\bar{1}\,0$] direction. (d) Clumps of Ir atoms form bridge-like structures (arrows) between Ir islands.

The distribution of Ir adatoms in relation to multilayer Ir islands is quite interesting. Long, slender clumps of Ir atoms form between many medium-sized islands. Examples of these “bridge”

http://dx.doi.org/10.1016/j.susc.2017.08.021

structures are highlighted with black arrows in Figure 3d, which shows island growth near a step edge, with part of the image differentiated to enhance contrast. The dimensions of the bridges are ~2-10 Ir atoms in width and up to 15 nm in length. This is a new form of growth which has not been previously observed for other systems.

Differentiating part of the STM images is helpful in distinguishing small features (Figs. 3c, 3d). Figures 3b and 3d also show that Ir atoms show a preference for collecting at substrate step edges. Clumps of bright protrusions are located at the upper edges of the steps in the STM images shown in Fig. 3bd. Ir double-layer islands show a slight preference for situating on the lower edges of steps, though they are clearly found on upper edges of steps and all throughout terraces (Fig. 2ef).

A more recent, high resolution STM study of Ir on Ge(111) shows features on both the Ir islands and on the substrate have √3 spacing.[26] Thus the large terraces of the Ge substrate appear to have a √3 reconstruction that is induced by the deposition of Ir, although we cannot determine whether the terraces are composed mostly of Ge or of Ir-Ge alloy. This explains the occurrence of sharp √3 LEED patterns, despite the small area covered by Ir islands. In fact, √3 reconstructions have previously been observed on both clean Ge(111) and Si(111),[28-30] prior to the formation of the well-known c(2x8) and 7x7 reconstructions, respectively.

The same high resolution STM study explained the origin of the bridge structures that connect the Ir islands.[26] The bridges were determined to follow the antiphase domain boundaries between competing surface domains of the Ge $\sqrt{3}$ surface reconstruction.

Ir deposition carried out at several temperatures between 340 and 500°C all yielded similar results in LEEM and LEED images. The LEED pattern showed evidence for √3 Ir growth, but domain sizes were too small to resolve in LEEM images. However, deposition of 1.2ML of

http://dx.doi.org/10.1016/j.susc.2017.08.021

Ir at RT did not produce a significant change from the clean Ge(111) LEED pattern. The LEEM image also remained unchanged for room temperature Ir deposition, with the exception of a gradual decrease in the sharpness of substrate step contrast during deposition.

3.3. Annealing Ir/Ge(111) deposited at low temperature and at low coverages

Increasing the sample temperature after room temperature Ir deposition resulted in the appearance of √3 spots in the LEED pattern (data not shown), as well as islands of √3 Ir in LEEM images (Fig. 4). Figure 4a shows a LEEM image of the Ge(111) surface after deposition of 1.2ML of Ir at room temperature. The LEEM image appears virtually unchanged from images of the surface before Ir deposition. Ir spots became apparent in the LEED pattern after increasing the temperature to 350°C. The intensity of √3 spots further increased as the sample temperature was increased to 460°C, although ordered regions of Ir were still not visible in the LEEM image (Fig. 4b), presumably because the domains were too small to resolve. The sample temperature was further increased while monitoring the LEEM image. By 610°C, bright domains of Ir √3 were clearly discernible, with island sizes <50 nm (Fig. 4c). Ostwald ripening was observed as the temperature was further increased to 720°C, as islands of √3 Ir increased in size to ~30-200 nm in diameter, with roughly spherical shapes, and decreased in number density (Fig. 4d).

Ostwald ripening of Ir √3 islands continues as the sample is heated to 830°C, the temperature at which √3 islands begin to disappear from the surface. LEEM images show that six-sided islands begin to grow as √3 islands disappear from the surface. Figure 5 presents a series of LEEM images in chronological order as the sample temperature was raised above 830°C. The sample surface in Figure 5a was prepared by depositing 1.2ML of Ir deposited at 350°C and then annealing to 670°C. Small bright dots in the LEEM image correspond to small islands of √3 Ir. As the sample temperature is increased beyond 830°C, expanding circular regions of bare Ge begin forming at multiple locations on the surface (Fig. 5b). A dark, six-sided island is located at the center of each expanding circular region of Ge. Circular regions of bare Ge continue to expand (Fig. 5cd), depleting the √3 Ir phase. If the temperature is reduced below 830°C while Ir is still present on the surface, the process of eliminating the √3 Ir phase stops; otherwise, this process continues until all of the √3 Ir phase on the surface completely disappears, leaving only the dark hexagonal islands (Fig. 5e). Multiple Ar^+ sputtering cycles were required to remove the hexagonal islands from the surface, as annealing alone up to 900°C did not remove them. Thus, these islands are strongly bonded to the surface and may be composed of Ir_xGe_y alloy structures, as discussed in more detail below.

During the high temperature phase transformation from √3 Ir to hexagonal islands, the shape of the retreating √3 Ir domain boundaries suggests that hexagonal island growth may act as a sink for Ir atoms as they diffuse away from the edges of √3 domain boundaries. As hexagonal islands grow, a region of bare Ge expands in a circular shape around each island (Fig. 5bcd), until eventually the surface is composed of only hexagonal islands and Ge (Fig. 5e). The LEED pattern corresponding to the surface after the √3 phase is no longer present only contains diffraction spots associated with Ge(111), including weak features associated with the (2x1) reconstruction (Fig. 5f), supporting identification of the area surrounding hexagonal islands in LEEM images as Ge.

Surface Science **666 (2017) 96–103**
http://dx.doi.org/10.1016/j.susc.2017.08.021

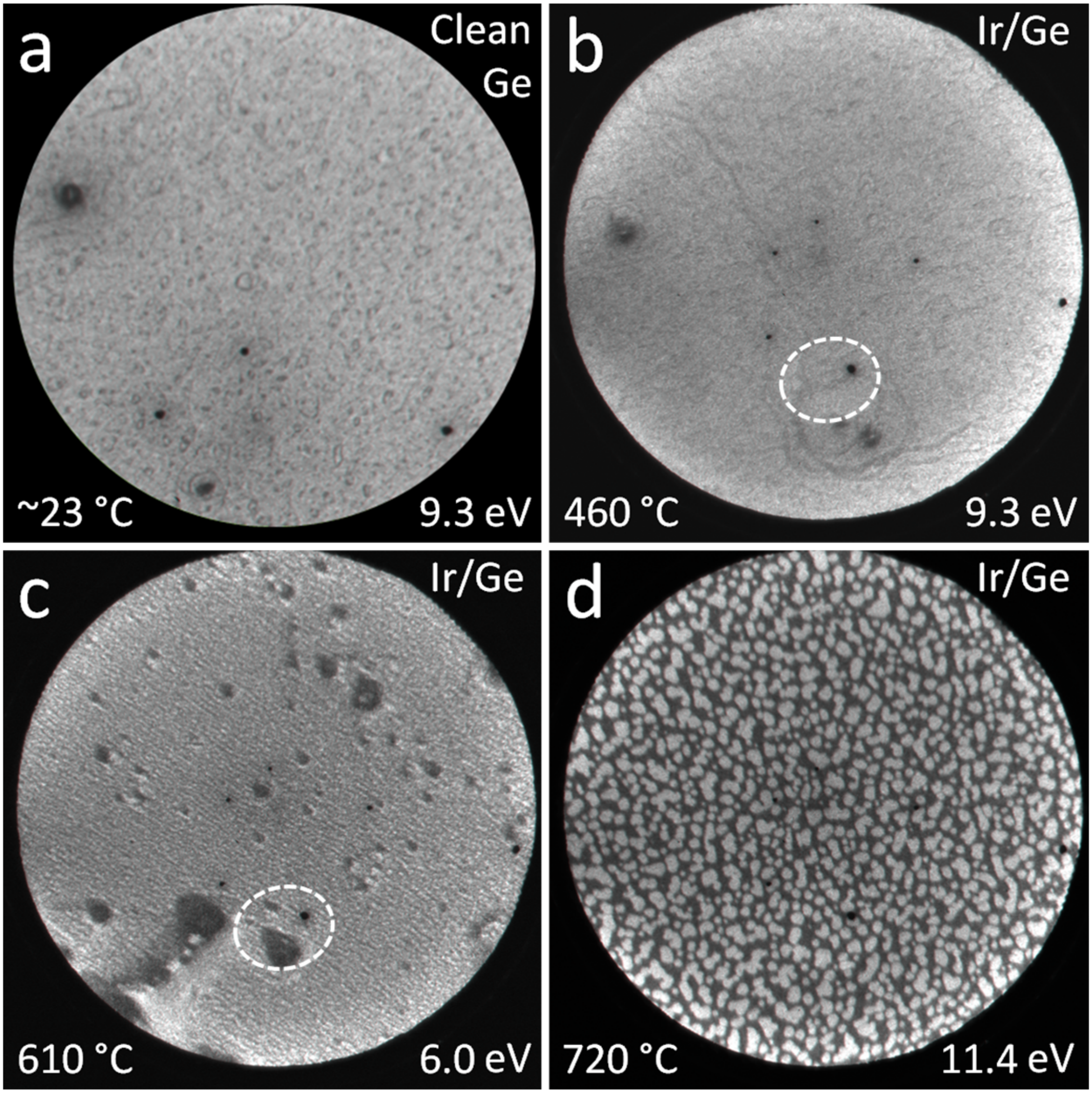

FIG. 4. LEEM images of 1.2ML of Ir deposited on Ge(111) at room temperature (RT), followed by annealing to 720°C. The oval feature of increased intensity outlined with a dotted line in (b) and (c) is a temporary feature caused by an overexposure of the microchannel plate and does not correspond to any feature on the sample surface. (a) Ge(111) surface before deposition. Contrast seen is due to high step density of substrate as well as large defects with dark contrast. The cratered texture of the surface is the same as was observed in LEEM images of the clean surface before Ir deposition and is due to sputter damage accumulated over many cleaning cycles performed with Ar^+ ion sputtering. Three deep black spots in lower half of image are channel plate defects. (b) After deposition of 1.0ML Ir at room temperature, followed by annealing to 460°C. Although √3 LEED spots are clearly visible (not shown), Ir islands are still too small to resolve in LEEM images. (c) After annealing to 610°C, small islands of Ir (bright) are clearly visible. Large dark structures are due to defects in a rough area of the surface, in a different area from that shown in the other three images. (d) Ostwald ripening between 610°C and 720°C produces large islands of Ir (bright). 5 µm field-of-view (FOV).

http://dx.doi.org/10.1016/j.susc.2017.08.021

While we cannot rule out the possibility that Ir desorption happens alongside the formation of the hexagonal islands as the √3 Ir phase disappears from the surface above 830°C, a simple estimate of the average height of hexagonal islands seen in LEEM images, assuming all Ir in the √3 phase ends up in hexagonal islands, is consistent with the heights of hexagonal islands measured with STM (discussed below). A height estimate was performed for an image from the same sequence as those in Figure 5 and similar to that shown in Figure 5e. For that image, hexagonal islands were found to occupy 2.0% of the surface area, and the coverage was 1.2ML of √3 Ir. In addition to using our calibrated Ir coverage, we make the following three assumptions: (1) no desorption of Ir, (2) no hexagonal islands too small to observe in LEEM, and (3) the hexagonal islands seen in LEEM are composed entirely of Ir(111) with a square height profile. We then find that the average island height is 6.2nm.

The composition of six-sided islands formed at high temperature is unknown, although two studies have identified mixtures of several Ir_xGe_y compounds for Ir deposited on Ge and annealed up to 800°C.[17, 18] The LEED pattern from this surface shows only spots from the clean Ge(111) high temperature surface, with neither remaining √3 Ir features nor extra spots that might be attributed to the dark hexagonal islands (Fig. 5f). These islands are dark at all LEEM imaging energies, which may indicate some internal disorder. They are readily distinguishable from the √3 Ir phase, as well as from other ordered monolayer reconstructions which typically show significant intensity variation with imaging energy. Although the six-sided islands are similar in size to some of the substrate defects that were present in LEEM images of every clean Ge(111) sample investigated, they have faceted edges which distinguish them from substrate defects, which have rounded edges. Similar hexagonal islands were observed for high temperature Ir deposition above 2.0ML and are discussed further below.

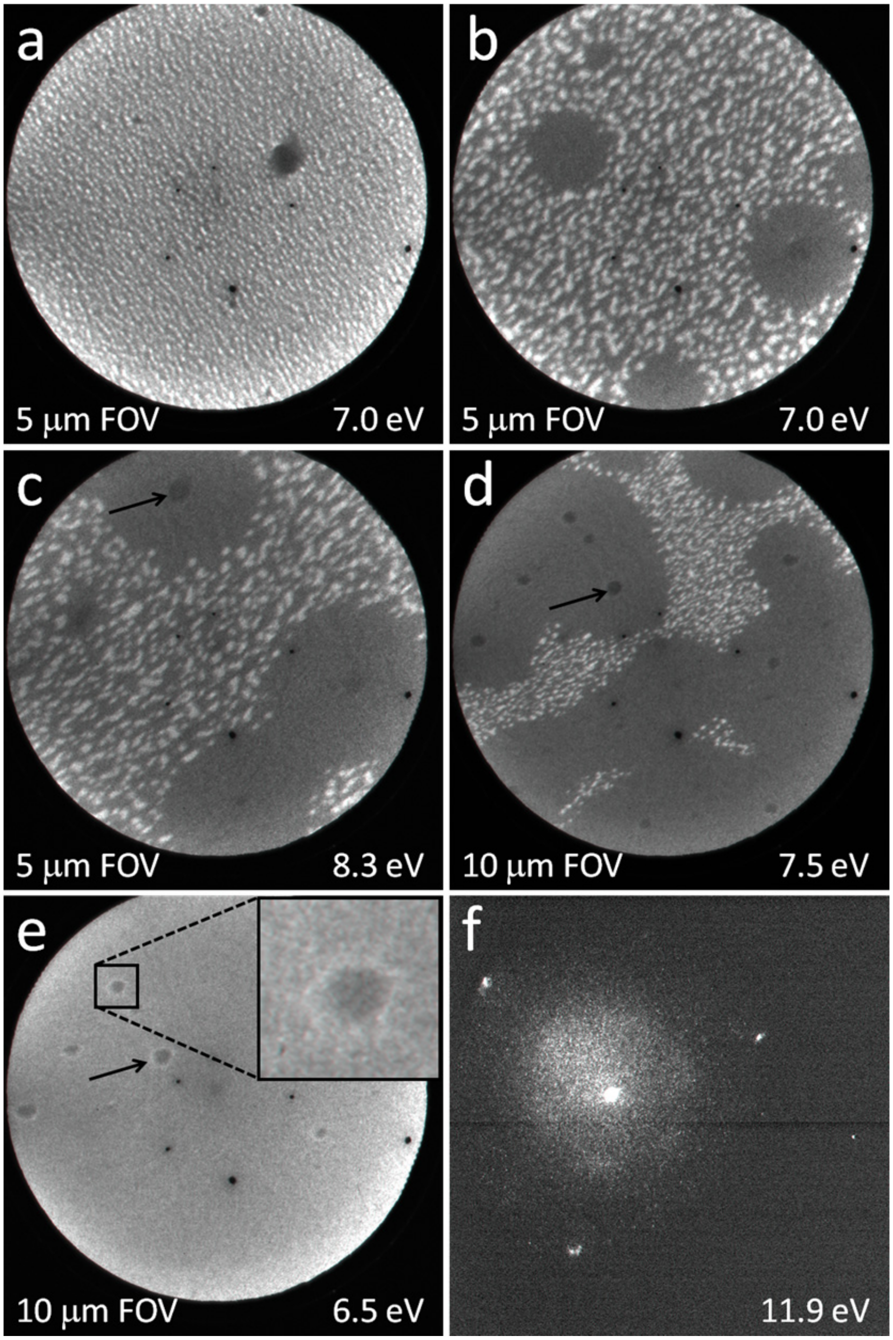

FIG.5. Upon heating 1.2ML of Ir beyond 830°C, LEEM images show elimination of √3 Ir islands in favor of hexagonal multilayer islands. Images are presented in chronological sequence. For reference, a black arrow points to the same hexagonal island in three different images. If the sample shown in (e) is cooled below 830°C to room temperature, the shapes and sizes of hexagonal islands remain unchanged in LEEM images. The LEED pattern in (f) corresponds to the surface shown in (e), after the sample has been allowed to cooled to 80°C. (a) After original deposition at 350°C, 1.2ML of Ir was annealed to 670°C. Small bright islands are √3 Ir. (b)-(d) Upon heating beyond 830°C, circles of bare Ge expand around dark hexagonal islands, depleting the √3 Ir phase. (e) After √3 Ir is depleted, the hexagonal islands (inset) remain (f) LEED confirms that √3 is no longer present on the surface. The only LEED spots remaining are first order Ge(111) spots (four of which are visible in this image) and features associated with the Ge(111) (2 x 1) reconstruction.

3.4 Growth of Ir on Ge(111) between 650 and 820 °C

Ir deposited on Ge(111) samples held at temperatures between 650 and 820°C showed the occurrence of the Stranski-Krastanov growth mode, with one layer of the √3 Ir phase forming, followed by the formation of small multilayer islands. Figure 6 shows a sequence of LEEM images taken in chronological order as 2.6ML of Ir were deposited on Ge(111) at 700°C; the movie from which these images were taken is available as supplemental material for this paper.[31] Within a 10 μm LEEM FOV, the √3 Ir phase nucleates on multiple areas of the sample (Fig. 6a). Ir islands have dendritic arms with smooth edges (Fig. 6b). Figure 6b also shows that island growth is bounded by substrate step bunches, which run between the lower left and upper right of the images in Figure 6. The presence of numerous long, thin √3 islands that are roughly oriented along a line running between the lower left and upper right of the LEEM image in Figure 6b may be attributed to island elongation parallel to substrate step bunches. In Figure 6c, the Ir growth seems to be approaching the percolation threshold, where the Ir islands have joined into one interconnected network. By Figure 6d, the Ir has nearly formed one layer, with the steps of the original substrate still evident. Figure 6e shows completion of the layer, with small dark features evident, presumably corresponding to multilayer islands. In Figure 6f, many dark multilayer islands can be seen, with compact shapes and somewhat rounded edges. The area of the surface covered by the dark compact islands in Figure 6f is ~7%. Given the 2.6ML coverage for this image, we estimate that the height of these islands averages 8 to 9 layers.

***Surface Science* 666 (2017) 96–103**
http://dx.doi.org/10.1016/j.susc.2017.08.021

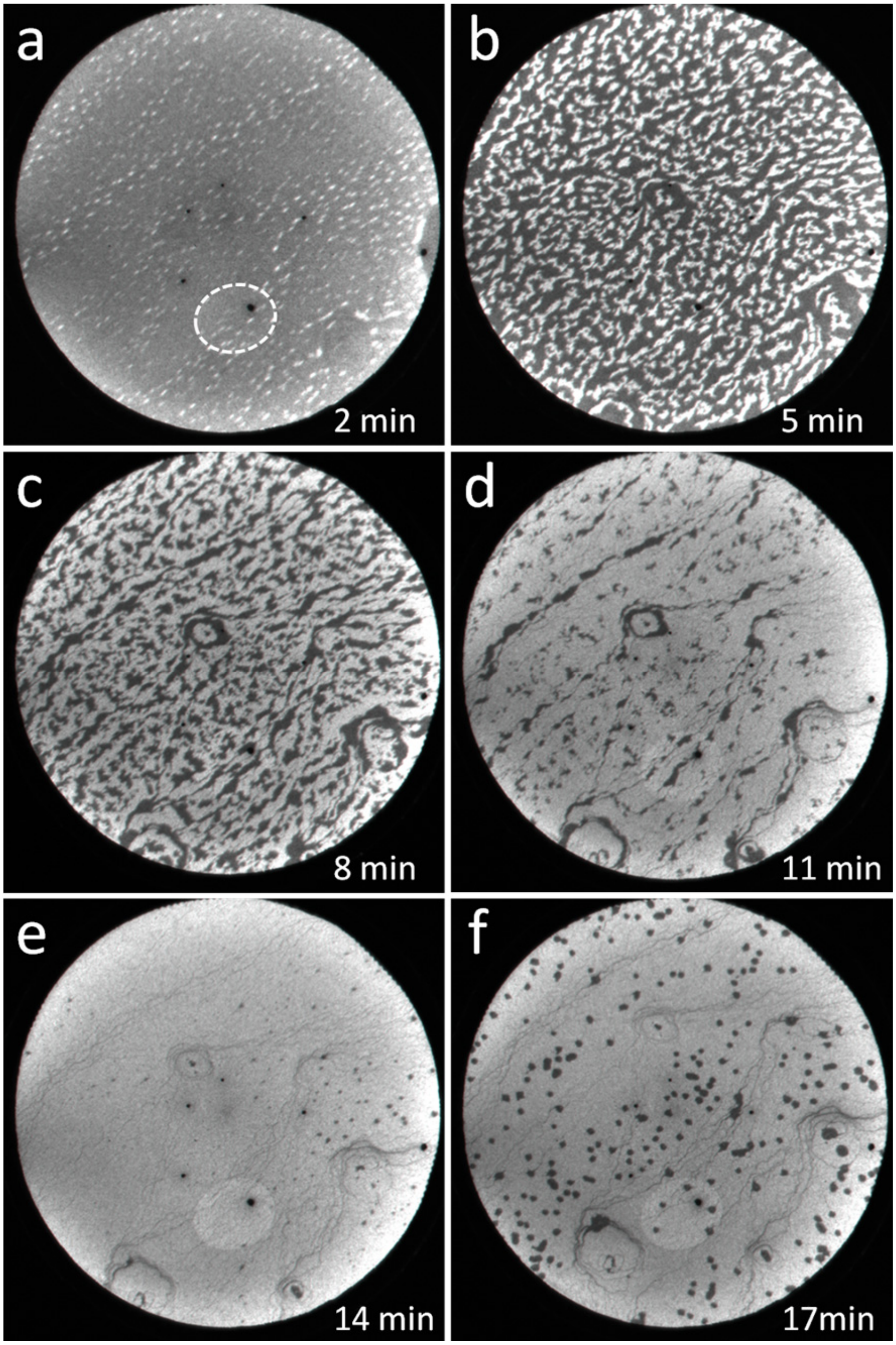

FIG. 6. LEEM images of deposition of 2.6ML of Ir on Ge(111) at 700°C, as a function of the deposition time in minutes, as labeled on the figures; the movie from which these images were taken is available as supplemental material for this paper.[31] The √3 Ir phase is bright in all images. The first √3 layer (2.0ML) completes near 13 min of deposition. Before 13 min dark areas of the sample are Ge, but dark areas of the sample at 14 min and 17 min are multilayer Ir islands. The oval feature of increased intensity outlined with a dotted line in (a), and also noticed prominently in (d,e,f), is a temporary feature caused by an overexposure of the microchannel plate and does not correspond to any feature on the sample surface. E = 6.0 eV. FOV = 10 μm.

***Surface Science* 666 (2017) 96–103**
http://dx.doi.org/10.1016/j.susc.2017.08.021

After the completion of the √3 layer, multilayer island growth is apparent in LEEM images as small dark circles at 7.0 eV imaging energy (Fig. 6f). Imaging at 3.3 eV (Fig. 7a) or 7.6 eV (Fig. 7b) shows that two distinct phases are present, apart from the √3 Ir region. At the center of each circle is a small dark six-sided island (Fig. 7). Although most islands appear more triangular than hexagonal, a close examination reveals that they have six sides (Fig. 7b, inset). The variation in LEEM intensity of these hexagonal islands with energy is minimal; they have relatively dark contrast compared to other surface phases at all energies examined from 0 to 80 eV. However, the relative intensity of the regions surrounding hexagonal islands varies significantly with imaging energy. Surrounding each hexagonal island is a region with bright contrast at 3.3 eV, brighter than both the surrounding √3 Ir phase and the hexagonal islands. We do not know the structure of the phase that surrounds the hexagonal islands because no new LEED spots accompany the formation of this phase, which could be a second layer of Ir or a Ge-Ir alloy.

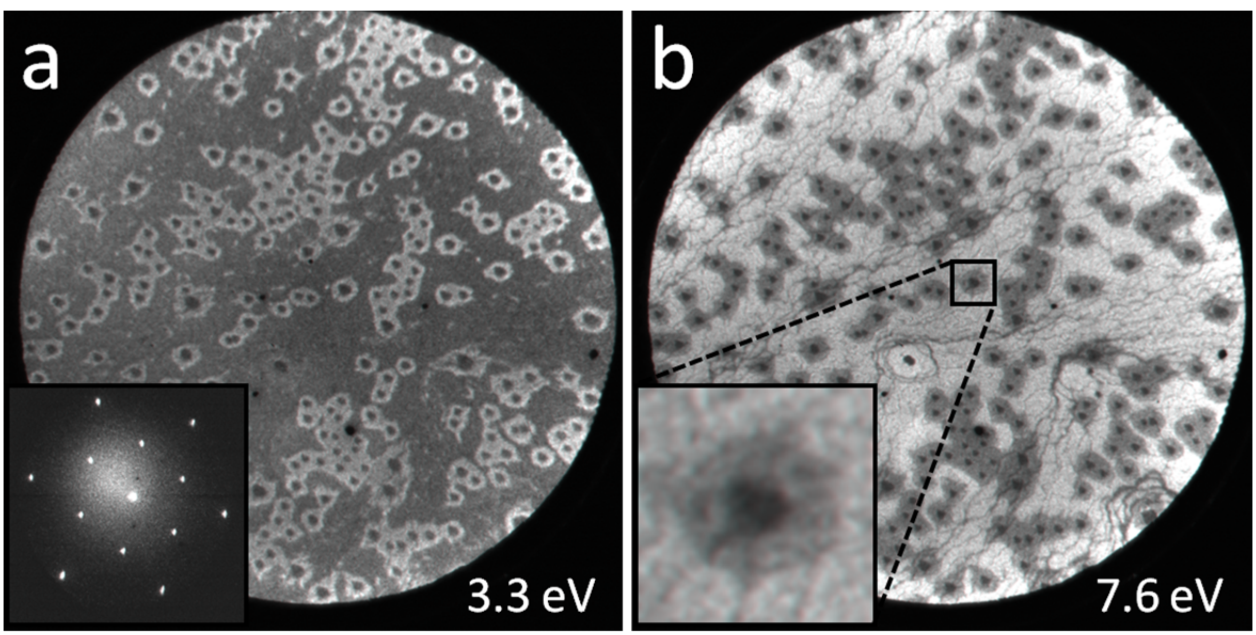

FIG. 7. Variation in contrast with imaging energy for 2.6ML of Ir on Ge(111) deposited at 700°C. FOV = 10 μm. (a) At an imaging energy of 3.3 eV, small black islands in the center of bright circles are multilayer hexagonal islands. Inset shows the LEED pattern corresponding to this surface is √3 Ir. (b) As the imaging energy is increased to 7.6

eV, the contrast of the hexagonal islands changes little, while the contrast between the √3 Ir phase and the regions surrounding hexagonal islands reverses near 5 eV imaging energy. Inset magnifies the indicated 700 nm^2 region, which includes one six-sided island (black) and surrounding phase (dark grey) that is distinct from Ir √3 (light grey).

The growth of Ir on Ge(111) at 650°C was similar to that observed at 700°C. For deposition of more than one layer of Ir, small hexagonal islands formed, each surrounded by a separate phase distinct from √3 Ir. The shape of the region surrounding the hexagonal islands was affected by the step density of the substrate. In a relatively flat region of the sample, the shape was roughly circular (Fig. 8a). In a region of the surface with numerous step bunches, the shape was elongated in the direction of steps (Fig. 8b). That growth is elongated along steps shows that steps form a barrier to growth, although the barrier is not absolute, as single domains of this phase do cross steps (Fig. 8b).

Annealing to a temperature above 830°C causes the dark regions surrounding the hexagonal islands to increase in size as the √3 phase retreats (Fig. 8c). That the area of the phase that surrounds hexagonal islands increases upon sample heating, as well as increasing upon further Ir deposition, again suggests that it is composed of either ordered or disordered Ir or Ir_xGe_y.

Figure 8d shows an STM image of the sample for which the LEEM image is shown in Figure 8c. While the STM resolution in this image is not adequate to identify atomic structure, smooth step edges suggest the presence of Ir (Fig. 8d). In contrast, step edges on clean Ge(111) are ragged and pointy at nm length scales. Figures 8d shows ragged step bunches with a smooth-edged overlayer, which may be due to the Ir √3 phase, extending just up to the edges of steps. Hexagonal islands observed with LEEM were also observed with STM. An STM image of one hexagonal island is included as an inset in Figure 8d. The height of the island was measured at

7.0 nm, which is very close to the LEEM estimate of 6.2nm described above. Islands observed with STM were all located at substrate step edges, with the tops of islands being somewhat flat.

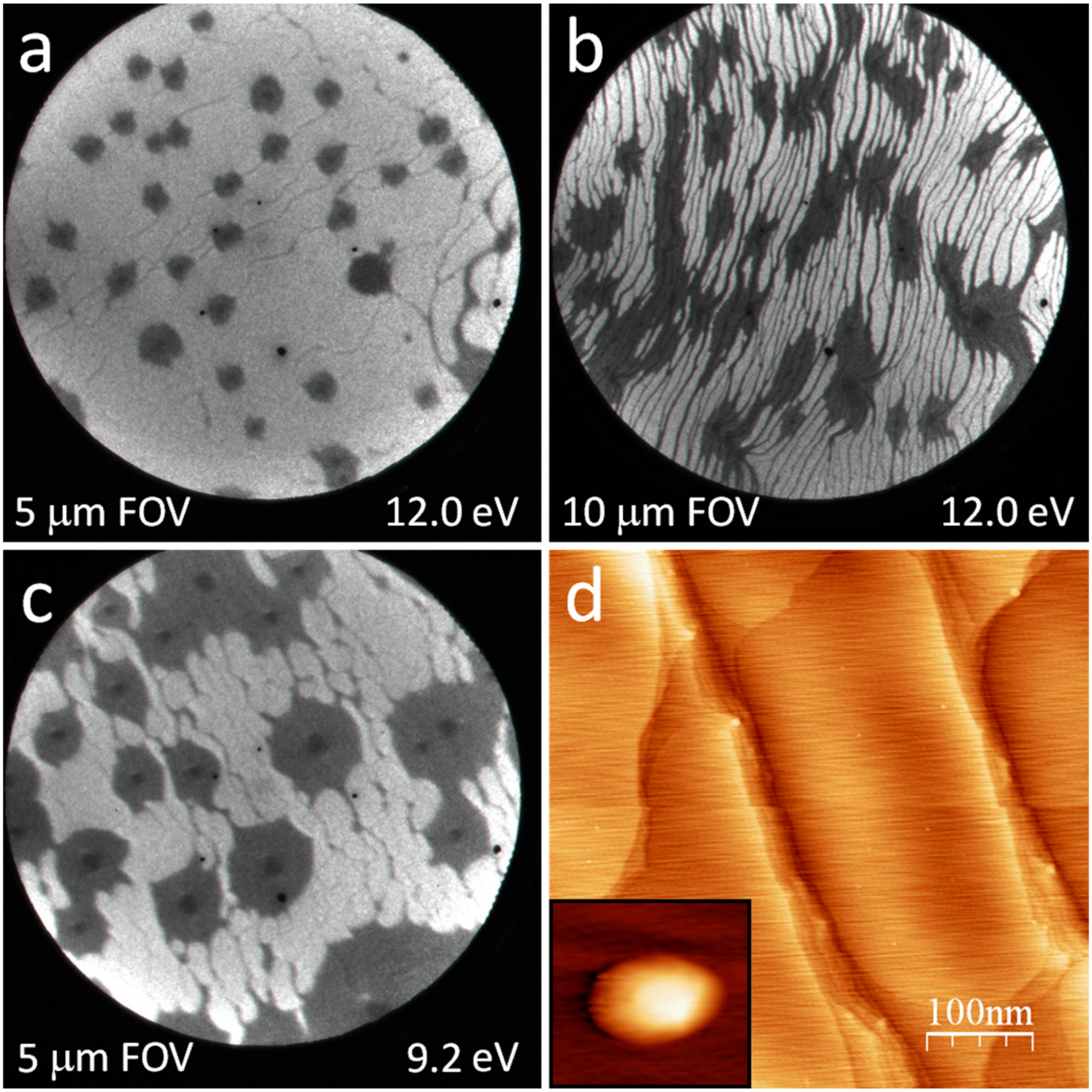

FIG. 8. (Color online) LEEM and STM images of deposition of 2.4ML of Ir on Ge(111) at 650°C (a,b), and after briefly annealing to 880°C (c,d). Images are all from the same sample. (a) Dark circular regions are Ir growth after the completion of the √3 wetting layer (bright). Within each dark circular region there are two layers of contrast, indicating two different Ir phases. (b) Stepped region of the sample. Dark regions of growth beyond the first √3 wetting layer are elongated in the direction of steps. (c) Dark regions surrounding Ir islands have increased after annealing to 880°C for several seconds while the operator monitors the LEEM image. (d) Rounded step edges in STM images suggest presence of Ir. The inset of a 53.2 x 50.0 nm region shows a multilayer island located near a step edge, but taken from a different STM image of the same sample. The height of the island is 7.0 nm. Sample bias= -2.0 V, tunneling current = 0.5 nA.

3.5. Annealing Ir/Ge(111) deposited at high temperature and high coverage yields Ir (3x1)

Upon heating above 830°C, the √3 phase in LEED images disappear. Only (1x1) spots remain above 830°C. When 2.6ML of Ir with √3 LEED pattern was heated to 830°C and then quickly cooled, we observed the formation of an Ir (3x1) phase (Fig. 9), with no √3 spots apparent. Figure 9 shows LEEM and LEED images of the surface after the sample, for which the LEEM image was shown in Figure 7b, was heated above 830°C and then rapidly cooled. In addition to the remaining hexagonal islands, two distinct phases are present on the surface: small domains of a phase with bright contrast interspersed with a phase that has intermediate contrast (Fig. 9a). The domain sizes of both phases are large enough (0.1-1 μm in diameter) to be well resolved in LEEM images. Both phases are spread across the entire surface, except near the hexagonal islands, where only the phase with intermediate contrast is found (Fig. 9a). The LEED pattern corresponding to this surface shows a distinct (3x1) pattern, with increased intensity for one of the three rotational domains (Fig. 9bc). It is also possible that this LEED pattern corresponds to a non-primitive (3x3) structure with subsets of spots with different overall intensity, due to internal structure of the unit cell. As clean Ge(111) does not form a (3x1) reconstruction, we attribute the (3x1) phase to Ir. Based only upon the bright-field LEEM images and LEED pattern, however, we cannot identify which of the two phases seen in Figure 9a is the (3x1) phase.

If the sample is heated again above 830°C, the (3x1) spots also disappear, but they return if the sample is cooled back below 830°C. Thus, this is evidence for a reversible phase transition at 830°C between the (3x1) and (1x1) phases.

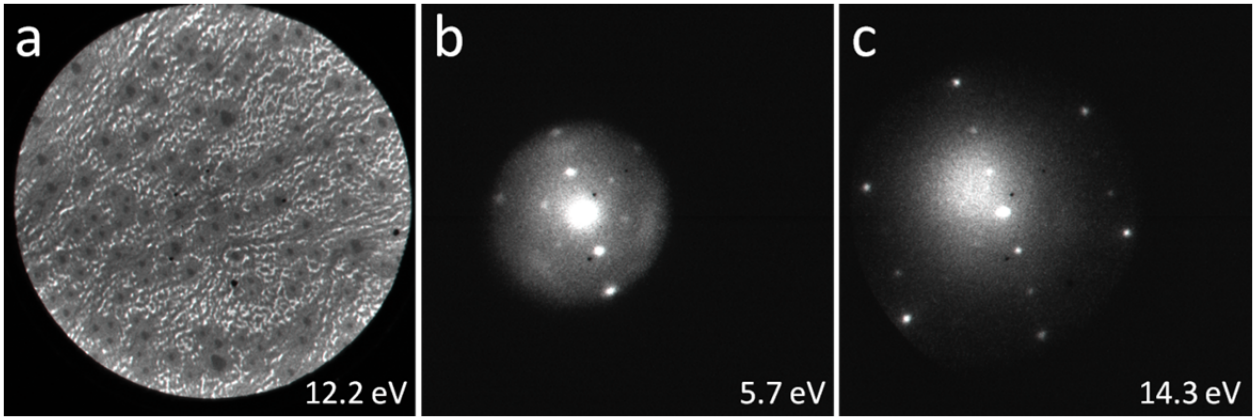

FIG. 9. LEEM and LEED images obtained after annealing 2.6ML of Ir (originally deposited at 700°C) to 830°C, followed by cooling to near room temperature. (a) LEEM image, 10μ FOV, showing hexagonal Ir islands remain on the surface (darkest contrast in image). Two other phases are present on the surface, a bright phase and a medium-bright phase. The medium-bright phase surrounds hexagonal islands. One of these two phases (the bright phase or the medium bright phase) likely corresponds to a (3x1) phase, as LEED images (b,c) show a (3x1) pattern, with one domain apparently brighter than the other two, particularly at the energy shown in (c).

4. Conclusions

This first surface study of Ir/Ge(111) revealed a pronounced difference between low temperature (≤500°C) and high temperature (≥650°C) growth of Ir on Ge(111). STM images of the Ir/Ge(111) surface resulting from Ir deposition at 350°C exposed a unique growth morphology with bridges of Ir atoms forming a network of connections between multilayer Ir islands. Sharp LEED patterns show evidence for a √3 phase. High resolution STM imaging shows that both the multilayer Ir islands and the large Ge terraces have √3 structure.[26] The lateral dimensions of the interconnected Ir islands ranged from ~10-20 nm, and the width of the bridge connections from ~2-10 Ir atoms.

Domain sizes of √3 Ir deposited at sample temperatures ≤500°C were too small to resolve in LEEM images. Annealing Ir/Ge(111) above 600°C, after deposition at a lower temperature, produced √3 islands large enough to resolve in LEEM. Ostwald ripening of √3 Ir islands was observed in LEEM images as temperature was further increased up to 830°C.

Ir deposition onto substrates at 650-820°C showed Stranski-Krastanov growth, with multilayer island growth following the completion of one layer of the √3 phase. Initial growth of the √3 phase had a dendritic morphology, and √3 islands had a "curly" shape. Substrate step edges act as barriers to √3 growth. Growth beyond 1 layer was in the form of hexagonal multilayer islands, with each surrounded by a region devoid of √3 Ir that is likely to be composed of disordered Ir or Ir-Ge alloy. Briefly annealing more than 1 layer of Ir to 830°C, followed by cooling the sample below 830°C, resulted in the elimination of √3 Ir from the surface and produced an Ir (3x1) phase. For Ir surface coverages of 1.2-2.6 ML, the √3 to (1x1) surface phase transition at 830°C was irreversible: the √3 structure did not return after cooling below 830°C. Once the (3x1) phase formed, however, it has a reversible phase transition to the (1x1) phase at the same transition temperature of 830°C.

Additional STM measurements on Ir/Ge(111) have already been performed to measure the structure of unusual island formations, such as dots, bridges, and islands, as a function of coverage and annealing temperature, giving insight into how these structures form on the surface.[26] In that study, an atomic model was presented, which is consistent with the XPS data presented here.

For future work, the several phase transformations observed in the LEEM movies merit further investigation. Micro-LEED measurements could be useful in determining additional structural information about the islands. Further STM studies of the higher coverage phases and of the hexagonal islands could also yield interesting insights into details of these structures.

***Surface Science* 666 (2017) 96–103**
http://dx.doi.org/10.1016/j.susc.2017.08.021

ACKNOWLEDGMENTS

The authors thank Charles S. Fadley for helpful discussions on fitting the Ir 4f XPS spectra and William R. Graves for the convolution program. The authors are pleased to acknowledge funding support from the National Science Foundation under Grants CHE-0719504 and PHY-1004848. The LEEM/STM/XPS instrumentation was funded by NSF DMR 9512231.

Surface Science **666 (2017) 96–103**
http://dx.doi.org/10.1016/j.susc.2017.08.021

References

[1] T. F. Mocking, P. Bampoulis, N. Oncel, B. Poelsema, and H. J. W. Zandvliet, Nat. Commun. 4, (2013) 5.
[2] N. Oncel and D. Nicholls, J. Phys.: Condens. Matter 25, (2013) 014010.
[3] Fatima, I. C. Oguz, D. Cakir, S. Hossain, R. Mohottige, O. Gulseren, and N. Oncel, J. Appl. Phys. 120, (2016) 095303.
[4] R. N. Mohottige and N. Oncel, Surf. Sci. 641, (2015) 237.
[5] S. A. Parikh, M. Y. Lee, and P. A. Bennett, J. Vac. Sci. Technol. A 13, (1995) 1589.
[6] D. Nicholls and N. Oncel, J. Phys.: Condens. Matter 25, (2013) 445004.
[7] M. Wittmer, P. Oelhafen, and K. N. Tu, Phys. Rev. B 35, (1987) 9073.
[8] S. J. Morgan, R. H. Williams, and J. M. Mooney, Appl. Surf. Sci. 56, (1992) 493.
[9] C. P. Ouyang, J. J. Chang, J. F. Wen, L. C. Tien, J. Hwang, and T. W. Pi, J. Appl. Phys. 91, (2002) 1204.
[10] N. Oncel, D. Çakır, J. H. Dil, B. Slomski, and G. Landolt, J. Phys.: Condens. Matter 26, (2014) 285501.
[11] A. Laszcz, A. Czerwinski, J. Ratajczak, J. Katcki, N. Breil, G. Larrieu, and E. Dubois, Archives of Metallurgy and Materials 51, (2006) 551.
[12] Y. S. Gong, C. B. Wang, Q. Shen, and L. M. Zhang, Appl. Surf. Sci. 254, (2008) 3921.
[13] Y. S. Gong, C. B. Wang, Q. Shen, and L. M. Zhang, Vacuum 82, (2008) 594.
[14] C. K. Chung, J. Hwang, T. H. Jaw, and D. S. Wuu, Thin Solid Films 373, (2000) 68.
[15] S. T. Prisbrey, S. P. Vernon, and W. M. Clift, J. Vac. Sci. Technol. B 23, (2005) 2378.
[16] P. Zuppella, G. Monaco, A. J. Corso, P. Nicolosi, D. L. Windt, V. Bello, G. Mattei, and M. G. Pelizzo, Optics Lett. 36, (2011) 1203.
[17] A. Habanyama and C. M. Comrie, Thin Solid Films 516, (2008) 5137.
[18] S. Gaudet, C. Detavernier, A. J. Kellock, P. Desjardins, and C. Lavoie, J. Vac. Sci. Technol. A 24, (2006) 474.
[19] C. L. H. Devlin, D. N. Futaba, A. Loui, J. D. Shine, and S. Chiang, Mat Sci Eng B-Solid 96, (2002) 215.
[20] E. C. Poppenheimer, *LEEM Data Analyzer software*, (2011).
[21] I. Horcas, R. Fernandez, J. M. Gomez-Rodriguez, J. Colchero, J. Gomez-Herrero, and A. M. Baro, Rev. Sci. Instrum. 78, (2007) 013705.
[22] I. N. Stranski and L. Krastanow, Abhandlungen der Mathematisch-Naturwissenschaftlichen Klasse IIb, Akademie der Wissenschaften Wien 146, (1938) 797.
[23] *CasaXPS: Processing Software for XPS, AES, SIMS and More*, http://www.casaxps.com/, (2016).
[24] D. A. Shirley, Phys. Rev. B 5, (1972) 4709.
[25] W. Smekal, W. S. M. Werner, and C. J. Powell, Surf. Interface Anal. 37, (2005) 1059.
[26] M. van Zijll, E. Huffman, D. Lovinger, and S. Chiang, Surf. Sci., (2017) in press.
[27] C. Kittel, *Introduction to solid state physics* (Wiley, 2005).
[28] W. C. Fan and A. Ignatiev, Phys. Rev. B 40, (1989) 5479.
[29] R. D. Meade and D. Vanderbilt, Physical Review B 40, (1989) 3905.
[30] W. C. Fan, A. Ignatiev, H. Huang, and S. Y. Tong, Phys. Rev. Lett. 62, (1989) 1516.
[31] *See suppplemental material at Surface Science website.*